First observation of γ-soft and triaxial bands in Zr isotopes

W. Urban,[1] T. Rząca-Urban,[1] J. Wiśniewski,[1] A. G. Smith,[2] G. S. Simpson,[2] and I. Ahmad[3]
[1]*Faculty of Physics, University of Warsaw, ulica Pasteura 5, 02-093 Warsaw, Poland*
[2]*Department of Physics and Astronomy, University of Manchester, M13 9PL Manchester, United Kingdom*
[3]*Argonne National Laboratory, Argonne, Illinois 60439, USA*

(Received 11 June 2019; published 26 July 2019)

New results obtained in this work from measurements of γ radiation following fission of ^{248}Cm and ^{252}Cf, performed using Eurogam2 and Gammasphere arrays, respectively, reveal excitations corresponding to γ vibrations and triaxial deformation present in ^{100}Zr and ^{102}Zr nuclei. This is the first observation of nonaxial bands in Zr isotopes. Such excitations probably occur due to competing prolate and oblate configurations, identified recently in these nuclei. Evolution of γ softness and triaxiality in Zr isotopes is observed in the function of the neutron number.

DOI: 10.1103/PhysRevC.100.014319

I. INTRODUCTION

Half a century after reporting strong, prolate deformation in even Zr isotopes with $N \geqslant 60$ [1], these nuclei can still surprise us. Our recent work [2] indicates that the structure evolution in these nuclei is more complex than just a prolate deformation occurring at $N \approx 60$. The nearly spherical 0_2^+ state in ^{100}Zr corresponds to an oblate configuration with a 2p-2h leading component, where a pair of neutrons is promoted from the $9/2^+[404]$ "extruder" to the $11/2^-[505]$ orbital, downsloping on the oblate side. The same $9/2^+[404]$ extruder lends two neutrons to the low-Ω orbital of the $\nu h_{11/2}$ shell, downsloping on the prolate side, producing the 0_1^+, ground-state configuration with a strong prolate deformation. The local appearance of the $9/2^+[404]$ orbital at $N \approx 60$ [3–6] explains the local presence of oblate configurations as well as the sudden increase of prolate deformation in ^{98}Sr and ^{100}Zr [2]. This local effect is superimposed on the gradual evolution of prolate deformation in the $50 < N < 66$, $36 < Z < 50$ region caused by the interaction of ground-state 0^+ levels with collective, excited 0^+ levels. The latter are 2p-2h, "intruder" configurations [7] due to the promotion of $d_{5/2}$ and $g_{7/2}$ neutrons to the $h_{11/2}$ shell, which then interact with proton particles or holes in the $g_{9/2}$ shell. The gradual evolution mentioned above may be interpreted in terms of intertwined quantum phase transitions proposed recently for Zr isotopes [8]. One should also mention here recent experimental work reporting prolate and oblate configurations coexisting in ^{99}Zr [9] as well as theoretical predictions of such an effect around ^{100}Zr [10].

The presence of prolate and oblate configurations close in energy suggests a nonaxial instability in these nuclei. This was considered in Ref. [11] for two-quasiparticle configurations, though another study [12] has presented arguments to the contrary. The subject deserves more attention because the axial asymmetry in Zr isotopes would resolve the puzzle of yet another sudden shape change in the region: the appearance of well-developed γ bands and triaxiality above $Z = 40$ in Mo [13,14] and Ru [15] isotopes. One would rather expect such an effect to develop gradually, starting at $Z = 40$, where the essential condition, the population of the $g_{9/2}$ orbital [16], is already fulfilled [16]. The present paper reports that this, indeed, happens in Zr isotopes.

In Sec. II we present the experiment and new experimental data, which are then discussed in detail to show the presence of γ and triaxial bands in ^{100,102}Zr. The paper is summarized in Sec. III.

II. EXPERIMENT, RESULTS, AND DISCUSSION

New data on ^{100}Zr and ^{102}Zr nuclei have been obtained from measurements of γ rays following spontaneous fission of ^{248}Cm and ^{252}Cf, performed using Eurogam2 [17] and Gammasphere [18] arrays, respectively. Both experiments were described in Refs. [19,20]. Multiple-γ coincidences obtained in these measurements allowed detailed excitation schemes of ^{100}Zr and ^{102}Zr to be constructed. In this work we present new data concerning triaxial and γ collectivity in both nuclei. The use of ^{248}Cm fission data made possible the identification of new transitions not reported in Ref. [21], where they were obscured by γ rays from the complementary fragments produced in fission of ^{252}Cf.

Figure 1 shows the partial excitation scheme of ^{100}Zr obtained in this work. The ground-state band and bands on top of the 331.32-keV and 2130.6-keV levels are drawn after Ref. [2], where previous studies of ^{100}Zr [11] are also discussed. Properties of γ lines and excited levels in ^{100}Zr, new compared to Ref. [2], are listed in Table I. Intensities of these transitions are in the same relative units as shown in Table II of Ref. [2], with the intensity of the 212.67-keV line normalized to 100. In the scheme we report a new band built on top of the 2244.7-keV level and new levels at 2208.5, 2471.8 and 2776.0 keV with their decays, as shown in Fig. 1. Together with the 1398.3- and 1856.2-keV, known levels [22] they form a cascade linked by the newly observed 304.5-,

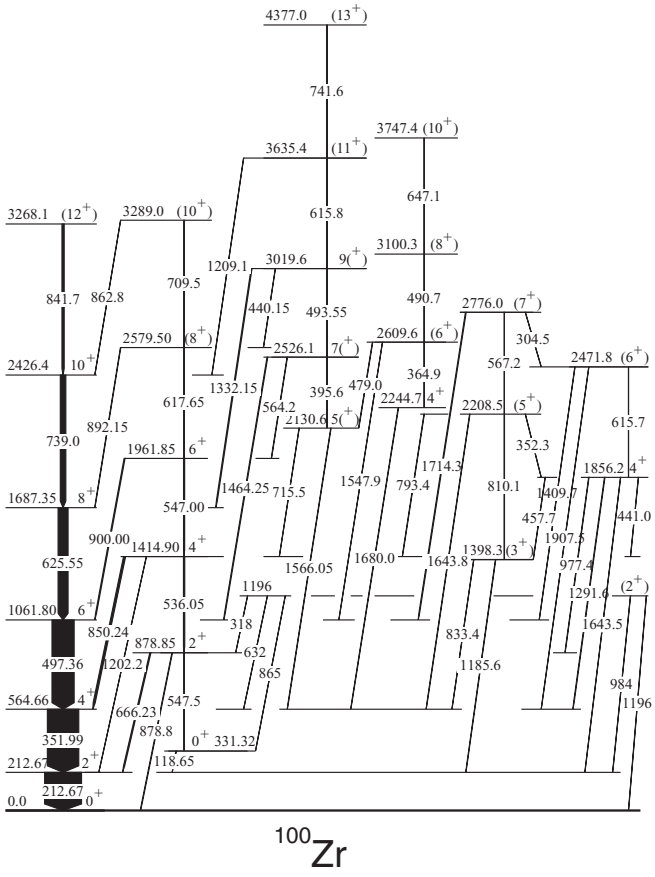

FIG. 1. Partial level scheme of ^{100}Zr, obtained in this work.

TABLE I. Energies and intensities of γ lines in ^{100}Zr and ^{102}Zr, as observed in this work in fission of ^{252}Cf or ^{248}Cm [labeled with a superscript *a*)].

E_γ (keV)	I_γ (rel.)	E_{exc} (keV)	E_γ (keV)	I_γ (rel.)	E_{exc} (keV)
	^{100}Zr			^{102}Zr	
212.67(3)	100(4)	212.67(4)	431.40(7)	3.2(2)	2093.4(1)
304.5(3)	0.2(1)	2776.0(3)	442.90(5)	1.4(2)	1829.35(8)
352.3(3)	0.4(2)	2208.5(2)	486.45(5)	55(2)	964.85(8)
364.9(1)	0.6(2)	2609.8(1)	498.10(5)	2.8(2)	2093.4(1)
441.0(3)[a)]	0.3(1)	1856.2(2)	531.7(1)	1.1(2)	2184.6(1)
457.7(2)	0.7(2)	1856.2(2)	533.45(5)	1.2(2)	2465.2(1)
479.0(2)	0.7(2)	2609.8(1)	545.3(1)	0.9(2)	2374.70(15)
490.7(1)	0.9(3)	3100.3(2)	570.6(1)	1.3(2)	2664.0(2)
567.2(2)	0.4(2)	2776.0(3)	630.50(5)	20(1)	1595.35(9)
615.7(2)	0.2(1)	2471.8(3)	641.0(1)	0.7(2)	2825.6(2)
647.1(2)	0.4(2)	3747.4(3)	658.6(2)	0.3(1)	3033.3(3)
793.4(2)	1.0(2)	2208.5(2)	667.8(2)	0.4(1)	3133.0(3)
810.1(1)	1.3(3)	2208.5(2)	697.05(5)	6.2(4)	1661.9(1)
833.4(2)	0.4(1)	1398.3(2)	705.4(2)	0.6(2)	3369.4(3)
977.4(1)	0.9(2)	1856.2(2)	756.45(5)	5.3(5)	2351.80(10)
1185.6(1)[a)]	1.7(3)	1398.3(2)	763.80(5)	2.0(3)	1242.20(5)
1291.6(1)	1.8(2)	1856.2(2)	860.4(1)	0.9(2)	3212.20(15)
1409.7(2)	0.5(2)	2471.8(3)	864.45(5)	1.9(2)	1829.35(8)
1547.9(2)	0.2(1)	2609.8(1)	869.80(5)	1.1(2)	2465.2(1)
1643.5(3)	0.4(2)	1856.2(2)	884.3(1)	4.2(5)	1036.4(1)
1643.8(1)	1.1(2)	2208.5(2)	891.1(1)	1.2(2)	1369.4(1)
1680.0(1)	0.7(2)	2244.7(1)	908.10(5)	4.1(3)	1386.50(7)
1714.3(1)	2.5(3)	2776.0(3)	966.90(5)[a]	2.8(3)	1931.8(1)
1907.5(2)	0.2(1)	2471.8(3)	1036.5(1)	1.8(2)	1036.4(1)
			1059.70(5)	2.2(2)	1538.10(8)
	^{102}Zr		1090.20(5)	17(1)	1242.20(5)
			1135.8(2)	1.1(3)	1287.7(2)
151.90(5)	100(4)	151.90(5)	1174.40(5)	3.1(3)	1652.85(7)
292.6(1)	0.8(1)	1661.9(1)	1183.5(1)	1.2(2)	1661.9(1)
326.50(5)	104(4)	478.40(7)	1217.4(3)	1.1(3)	1369.4(1)
350.3(1)[a]	0.7(1)	1386.50(7)	1219.8(1)	1.5(3)	2184.6(1)
393.8(1)[a]	0.5(1)	1931.8(1)	1230.2(1)	0.7(2)	2825.6(2)
410.7(1)[a]	0.4(1)	1652.85(7)	1409.9(1)	0.7(2)	2374.70(15)

352.3-, 457.7-, 567.2-, 615.7- and 810.1-keV transitions. The known (2^+), 1196-keV level with its γ decays [22] (not shown in Table I) is included to assist further discussion.

Summed angular correlation of the 1291.6-keV transition with two quadrupole transitions below in cascade, obtained from the ^{252}Cf data using the technique described in Ref. [23], is shown in Table II (we notice that only spins corresponding to the upper quadrupole transition are shown). It indicates spin $I = 4$ for the 1856.2-keV level, replacing the previous (6^+) assignment [22]. Positive parity is indicated by the large mixing ratio of the 1291.6-keV prompt transition and supported by the new 977.4-keV decay to the known 2^+, 878.85-keV level [2,22]. For other levels in this band we propose spins and parities based on decay branchings and the fact that the fission process populates predominantly yrast levels [24]. For the 1398.3- and 2208.5 keV levels we propose tentative spins 3 and 5, respectively, considering low-energy transitions linking these levels with the 1856.2-keV, 4^+ level. With spin $I = 5$ positive parity of the 2208.5-keV level is preferred, considering large δ of the 1643.8-keV prompt transition. Summed angular correlations of the 1680.0-keV transition in ^{252}Cf and ^{248}Cm data indicates spin-parity 4^+ for the 2244.7-keV bandhead. Again, the yrast population argument is used to propose tentative spins to other levels in this band.

Figure 2 shows the partial excitation scheme of ^{102}Zr with new bandheads and new spin-parity assignments to four excited bands reported partly in Refs. [21,25]. The 1036.4-keV level, first reported in Ref. [26], was interpreted in Ref. [21] as (2^+) bandhead of their band (8), comprising the 1242.2-, 1538.10- and 1793.3-keV levels. We do not confirm this band. As discussed in Refs. [12,27], the 1793.3-keV level is a two-quasiparticle (qp) configuration. The remaining levels are not linked by any "in-band" transitions and are assigned to other bands.

Part of the band on top of the 1036.4-keV level shown in Fig. 2 was reported in Ref. [21] as band (6) based on the 1386.50-keV level. The 350.3-keV transition linking the 1036.4- and 1386.50-keV levels is seen in ^{248}Cm fission data in a γ spectrum doubly gated on the 151.90- and 884.3-keV lines, shown in Fig. 3(a). Further gating confirms the location of the 350.3-keV transition in the scheme of ^{102}Zr, as shown in Fig. 2. Spin-parity 2^+ of the 1036.4-keV level is firmly assigned based on angular correlation in the

TABLE II. Experimental angular-correlation coefficients, A_k/A_0, for γ_1-γ_2 cascades in ^{100}Zr and ^{102}Zr, as observed in this work in fission of ^{252}Cf or ^{248}Cm, labeled *a*).

$E_{\gamma1}$-$E_{\gamma2}$	A_2/A_0	A_4/A_0	Spins	$\delta_{\rm expt}(E_{\gamma1})$
^{100}Zr				
1291.6-sum	0.018(33)	0.186(46)	3−4−2	No solution
			4−4−2	−2.8(7)
			5−4−2	No solution
1643.8-351.99	0.077(49)	0.003(69)	4−4−2	0.32(13)
			5−4−2	0.24(9), 3(1)
			6−4−2	Possible
1680.0-sum	0.064(32)	0.094(46)	4−4−2	−2.0(4)
			5−4−2	No solution
			6−4−2	No solution
1680.0-sum[a)]	0.111(35)	0.107(56)	4−4−2	−1.6(3)
			5−4−2	No solution
			6−4−2	No solution
^{102}Zr				
326.50-151.90	0.087(8)	0.001(12)	4−2−0	
486.45-326.50	0.103(8)	−0.001(12)	6−4−2	
630.50-486.45	0.089(14)	0.023(19)	8−6−4	
756.45-630.50	0.096(24)	−0.031(35)	10−8−6	
498.10-sum	−0.030(16)	0.011(23)	6−8−6	No solution
			7−8−6	−0.10(3)
697.05-sum	−0.082(18)	−0.022(27)	4−6−4	No solution
			5−6−4	0.04(3)
			6−6−4	No solution
763.80-326.50	−0.061(38)	−0.221(57)	2−4−2	No solution
			3−4−2	11(3)
			4−4−2	No solution
884.3-151.90	−0.028(22)	0.047(32)	1−2−0	No solution
			2−2−0	0.37(4),-5(1)
891.1-sum[a)]	−0.34(7)	0.07(9)	3−4−2	0.26(11)
			4−4−2	No solution
908.1-326.50	−0.051(24)	0.113(36)	3−4−2	No solution
			4−4−2	−5(2), 0.8(1)
			5−4−2	No solution
			6−4−2	No solution
966.90-sum	0.242(35)	−0.031(56)	5−6−4	−0.60(12)
			6−6−4	−0.26(3)
			7−6−4	0.97(5)
1059.70-sum	−0.010(23)	0.038(35)	3−4−2	−0.14(3)
			4−4−2	0.60(8)
			5−4−2	0.08(3)
			6−4−2	No solution
1090.20-151.90	−0.066(11)	−0.008(15)	2−2−0	No solution
			3−2−0	0.007(16)
			4−2−0	No solution
1174.40-sum	−0.049(31)	−0.068(46)	4−4−2	No solution
			5−4−2	0.03(5), 9(3)

884.3–151.90-keV cascade (large δ value excludes negative parity). Spin-parity 4^+ for the 1386.50-keV level is uniquely determined by angular correlations. We support tentative spin-parity assignments to higher-energy levels in this band proposed in Ref. [21].

The 1242.20-keV level is a new bandhead of the band reported in Ref. [21] on top of the 1652.85-keV level [their band (7)]. The 410.7-keV transition to the 1242.20-keV bandhead is seen in Fig. 3(b), in a γ spectrum doubly-gated on the 151.90- and 1090.20-keV lines. Spin $I = 3$ of the 1242.20-keV level is based on angular correlations. The directional-polarization measurement, using clover detectors of Eurogam2 as Compton polarimeters [28,29], yields linear polarization $P = -0.35(25)$ for the 1090.2-keV transition. Therefore, theoretical polarization of $-0.11(1)$ calculated for an $M1 + E2$ multipolarity indicates positive parity of the 1242.20-keV level.

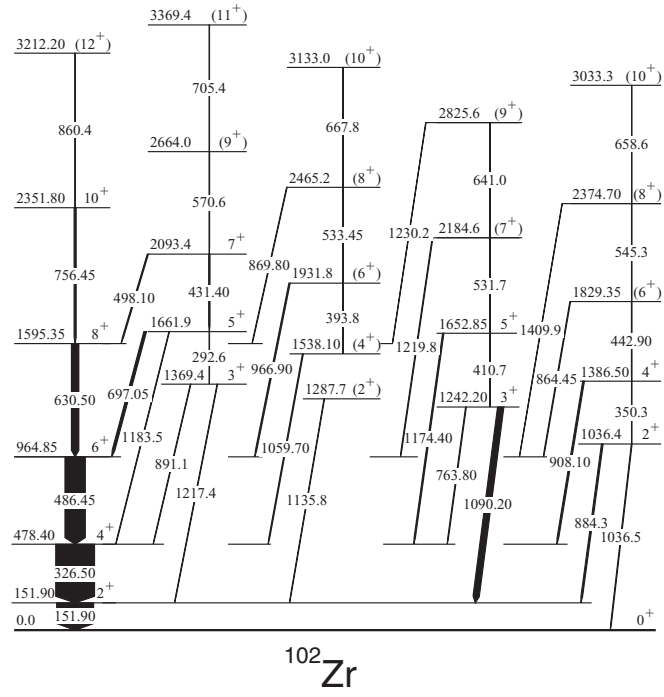

FIG. 2. Partial level scheme of ^{102}Zr, obtained in this work.

Angular correlations for the 1174.40-keV transition indicate spin $I = 5$ for the 1652.85-keV level, changing spin (6^+) proposed in Ref. [21]. Because of prompt 410.7-keV decay to the 3^+ level, parity of the 1652.85-keV level is positive. We notice that in fission of ^{252}Cf the 410.7-keV line is obscured by a strong, 409.9-keV line from ^{146}Ce, the complementary fission fragment to ^{102}Zr.

The 1538.10-keV level belongs to the band reported in Ref. [21] as band (4) on top of the 1931.8-keV level. The 393.8-keV decay from this level is seen in Fig. 3(c), in a γ spectrum doubly-gated on the (151.90+326.50)- and 1059.70-keV lines. We propose tentative spin-parity (4^+) and (6^+) for the 1538.10- and 1931.8-keV levels, respectively. Spin 8^+ assigned to the 1931.8-keV level in Ref. [21] is rejected by our angular correlations. The 1287.7-keV level, newly observed in this work, fits the excitation energy expected for the 2^+ head of this band.

Our angular correlations confirm spin $I = 5$ reported in Ref. [21] for the 1661.9-keV level. However, the experimental polarization $P_{\rm expt} = -0.36(22)$ of the 697.05-keV transition indicates its $M1 + E2$ multipolarity, for which the theoretical polarization is $P_{\rm th} = -0.15(1)$. Consequently, parity of

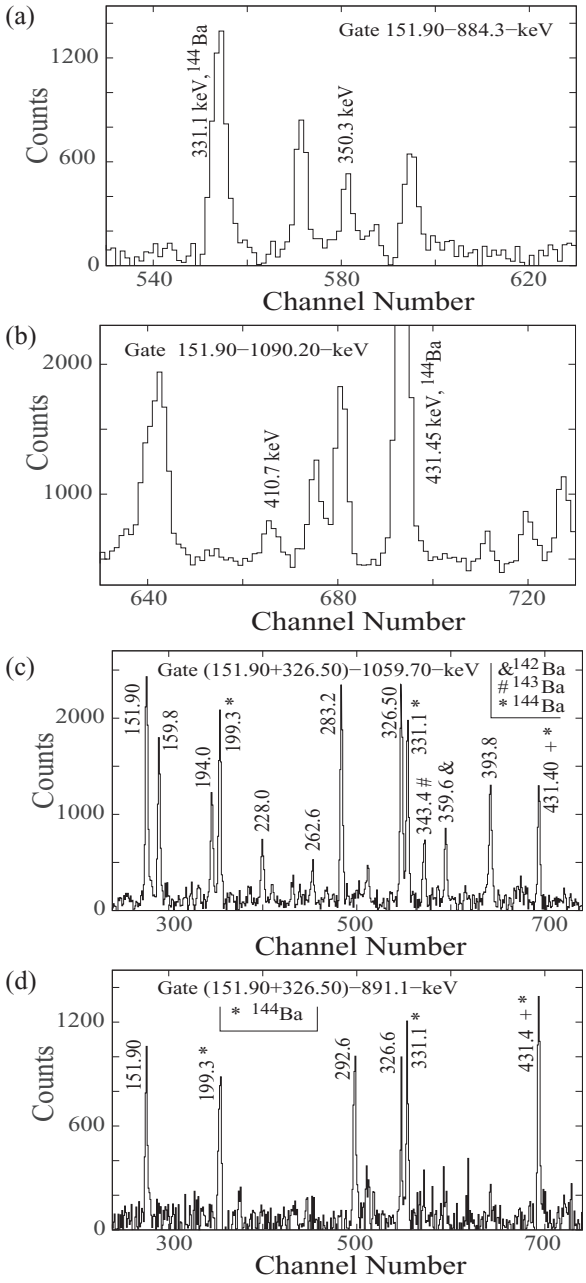

FIG. 3. Fragments of γ spectra, gated on lines of ^{102}Zr, as obtained from ^{248}Cm-fission data measured in this work.

the 1661.9-keV levels is positive. Angular correlations also indicate spin $I = 7$ for the 2093.4-keV level. Therefore, the 431.40-keV prompt transition is a stretched $E2$ and the parity of the 2093.4-keV level is positive. The 1661.9-keV level decays by the 292.6-keV transition, seen in Fig. 3(d), to the new 1369.4-keV level, which fits the excitation energy expected for the 3^+ member of this band. The 3^+ spin-parity is supported by angular correlations in the 891.1-sum cascade.

With bandheads below 1.4 MeV all four excited bands in ^{102}Zr, shown in Fig. 2, correspond to collective excitations. In ^{100}Zr the irregular cascade on top of the 1398.3-keV level is probably an emerging collective structure but bands on top

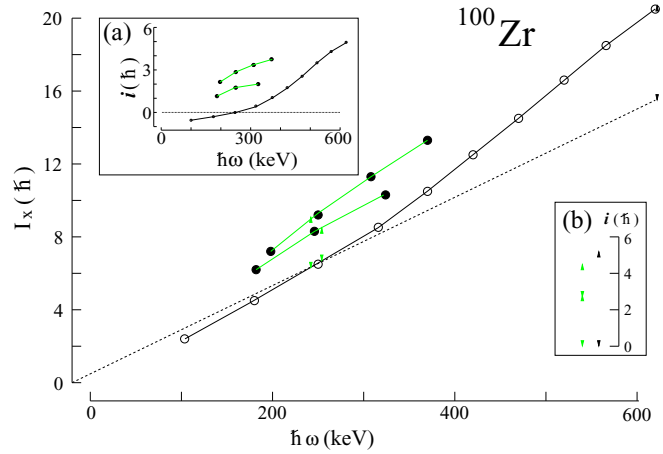

FIG. 4. Aligned angular momenta I_x and alignments i for bands in ^{100}Zr.

of 2130.6- and 2244.7-keV levels are probably admixed with 2-qp excitations.

Further insight into the structure of new bands in ^{100}Zr and ^{102}Zr can be drawn from Figs. 4 and 5 showing the aligned angular momenta of the new bands, defined as $I_x = \sqrt{I_i(I_i+1) - K^2}$, where I_i is the spin of the initial level, and the rotational frequency $\hbar\omega$ is defined as $\hbar\omega = [E(I_i) - E(I_f)]/2$, where $E(I_i)$ and $E(I_f)$ are excitation energies of the initial and final levels, respectively. Dashed lines in both figures serve as a references to estimate the alignment, i, defined as the difference between I_x and the reference. Reference lines in both figures are drawn through (0,0) and (6.25, 314) points on the $(I_x, \hbar\omega)$ plane, the latter located close to the data point for the $6_1^+ \rightarrow 4_1^+$ transition in both nuclei. Arrows in insets (b) in both figures are the same as in the main figure. The experimental data shown in Figs. 4 and 5 are taken from this work for low-spin levels and from Refs. [21,25] for high-energy levels with spins corrected to match our assignments at low energies.

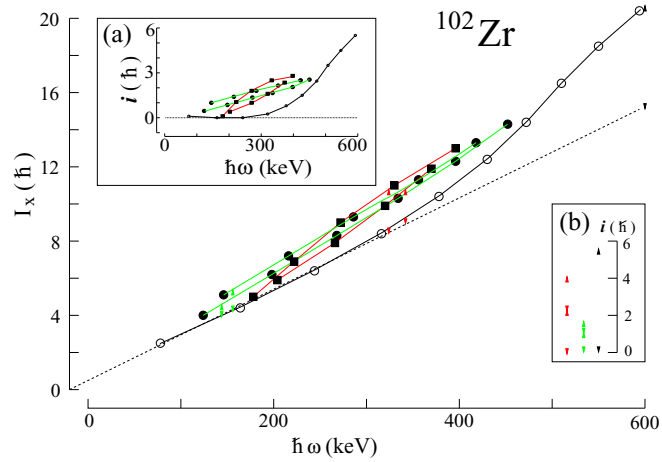

FIG. 5. Aligned angular momentum I_x and alignments i for bands in ^{102}Zr.

The $K = 0$, ground-state band of ^{102}Zr, represented by the black line (linking open circles) in Fig. 5 corresponds to a nearly rigid rotor up to pin $I = 8$. Above spin $I = 8$ the ground-state band gains alignment due to the aligning pair of $h_{11/2}$ neutrons [25]. Slow increase, extending over a wide range of rotational frequency suggests binding of this neutron pair to other particles. As illustrated in the inset (a) of Fig. 5 the final aligned angular momentum i in this band is probably higher than 7 $\hbar$.

The two bands on top of the 1287.7- and 1369.4-keV levels, represented by green lines (connecting full dots) in Fig. 5 correspond to a nearly rigid rotor. Similar character of their alignment plots suggest their common structure. The summed alignment at low spin in both bands, shown in the inset (b) of Fig. 5, is nonzero suggesting that these bands are two branches of a $K = 2$ collective structure with some admixture of a 2-qp configuration.

The alignment in the pair of bands based on the 1036.4- and 1242.20-keV levels, represented by red lines (connecting filled squares) in Fig. 5, grows from zero to $i \approx 2\hbar$ at $\hbar\omega \approx$ 400 keV in each band, suggesting for both bands a common, soft structure with $K = 2$. The picture is characteristic of an aligning phonon, by analogy to an octupole phonon alignment, which generates $i \approx 6\hbar$ (see Fig. 3 in Ref. [30]). Here, the summed alignment in both bands of $i \approx 4\hbar$ at $\hbar\omega \approx 350$ keV, shown in the inset (b) of Fig. 5, suggests a quadrupole phonon aligning.

The alignment process in the ground-state band of ^{100}Zr, shown by the black line (linking open circles) in Fig. 4, which is similar to that in ^{102}Zr, suggests similar configurations of ground-state bands in both nuclei. The ground-state band gains alignment due to the aligning pair of $h_{11/2}$ neutrons [25]. The gradual character of this alignment suggests binding of this neutron pair to other particles. As seen in the inset (a) of Fig. 4 the final aligned angular momentum i may be higher than $6\hbar$.

The initial alignment in bands on top of the 2130.6- and 2244.7-keV levels in ^{100}Zr, represented by green lines (connecting full dots) in Fig. 4 is about $2\hbar$ in each of them, which is more than in analogous bands in ^{102}Zr. Furthermore, these two bands are less regular than in ^{102}Zr, which suggests that their structures are less collective and mixed with two-quasiparticle configurations.

Further information can be obtained from the so-called staggering in bands. Figure 6 shows staggering $S(I)$ in ^{100}Zr and ^{102}Zr defined as

$$S(I) = \frac{[E(I) - E(I-1)] - [E(I-1) - E(I-2)]}{E_{\rm exc}(2_1^+)} \quad (1)$$

following Refs. [31,32]. $S(I)$ is often depicted as $S(I, I - 1, I - 2)$. In Ref. [33] detailed discussion of the staggering in various types of rotational structures in even-even nuclei is provided. The two most characteristic features of staggering are the "phase", telling whether $S(I)$ has higher value at even or odd spin values, and the amplitude of staggering between the minima and maxima of $S(I)$. A specific measure of the staggering discussed in Refs. [31–33] is the $S(4, 3, 2)$ value. For a γ-soft vibrator, $S(I) = -1$ for any spin I. For a deformed γ-soft structure, $S(4, 3, 2) = -2$ and $S(I)$ increases slowly with spin. For an axially symmetric rotor, $S(I) = +0.33$ independent of spin. For a γ-rigid deformed rotor with $\gamma = 30°$, $S(4, 3, 2) = +1.67$ and the staggering increases rapidly with spin. However, as argued in Ref. [34] neither of the "clean" solutions is realized in actual nuclei.

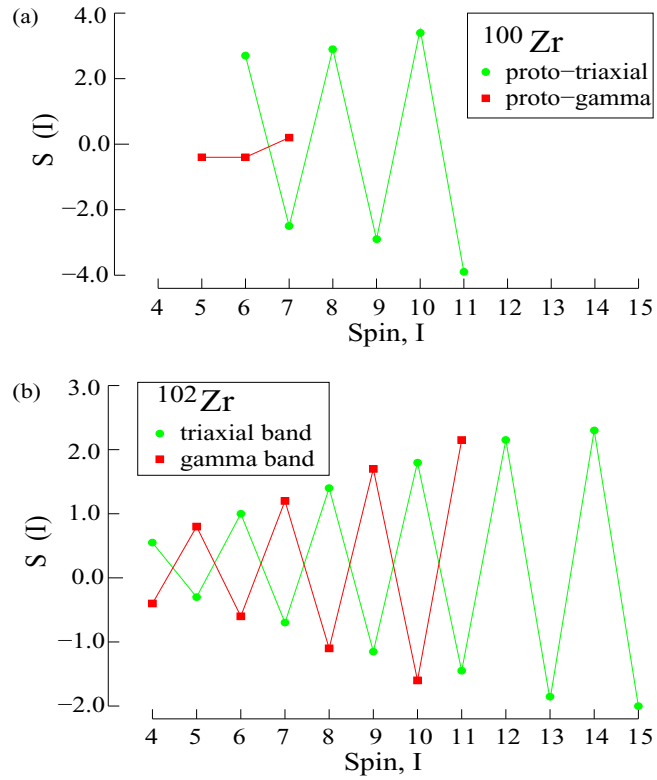

FIG. 6. Staggering in bands of ^{100}Zr and ^{102}Zr.

Staggering in the green bands of ^{100}Zr and ^{102}Zr (represented by filled circles), with minima of $S(I)$ at odd-I values, is characteristic of a rigid triaxial structure [33]. The amplitude of staggering in ^{102}Zr increases with spin suggesting a γ-rigid, triaxial band, though the $S(4, 3, 2) = +0.57$ value points to $\gamma < 30°$. In the green band of ^{100}Zr the phase is characteristic of a γ-rigid structure. The $S(4, 3, 2)$ value is not known but the staggering at low spins is clearly larger than in ^{102}Zr and rather constant. This suggests a nearly axially symmetric rotor structure of a 2-qp nature (a prototriaxial band) evolving into a triaxial rotor in the more collective ^{102}Zr isotope.

The staggering in the red band of ^{102}Zr (represented by filled squares), with minima of $S(I)$ at even I, is characteristic of a γ-soft structure [33]. Here $S(4, 3, 2) = -0.40$ and $S(I)$ increases with spin as fast as in the green band. This suggests a structure intermediate between the deformed γ-soft and deformed γ-rigid one. In ^{100}Zr the band emerging on top of the (3^+) level at 1398.3 keV shows at spin $I = 7$ an increase of $S(I)$ characteristic of a γ-soft structure. The band is not well developed and may be seen as a protoband evolving into a γ band in the more collective ^{102}Zr nucleus. We note that the absence of $\Delta I = 1$, in-band transitions in well developed $K = 2$ bands of ^{102}Zr is consistent with their proposed interpretation as γ-unstable structures.

In ^{100}Zr the green and red bands decay to both the ground-state band and the band on top of the 0_2^+ level at 331.22-keV. In Ref. [2] we proposed that the leading component of both configurations is a pair of neutrons in the $h_{11/2}$ shell, occupying low-Ω orbital in the ground-state structure and the 11/2[505] orbital in the 0_2^+ structure. The observed decays to both structures support this picture.

Finally, we discuss levels in ^{100}Zr and ^{102}Zr nuclei, which are not fully explained. The (2^+) level at 1196 keV may belong to the emerging γ-soft structure in ^{100}Zr, though we could not find the link to the 4^+, 1856.-keV level. One may also expect a 2^+ level in ^{100}Zr corresponding to the head of the emerging triaxial structure. Possible candidates with excitation energies around 1.9 MeV can be found in the compilation [22], but dedicated studies of low-spin levels in ^{100}Zr are needed to find the solution. In ^{102}Zr the 1287.7-keV level requires confirmation of its proposed bandhead role. Furthermore, two low-spin levels reported at 1159.50 and 1211.05 keV [35] need an explanation. With such low energies they are, most likely, collective excitations. Energy-wise, the two levels might be even seen as extensions by two units down in spin of bands on top of 1287- and 1369.0-keV levels, respectively. However, the 1159.50-keV level cannot be a 0^+ bandhead because it decays by a γ transition to the 0^+ ground state [35]. It is also unlikely that the 1211.05-keV level is a 1^+ bandhead, as such configurations are not expected in even-even nuclei at low energy.

III. SUMMARY

In summary, multiple-γ coincidences obtained from measurements of γ rays following spontaneous fission of ^{248}Cm and ^{252}Cf, performed with Eurogam2 and Gammasphere arrays, revealed the existence of new collective bands in ^{100}Zr and ^{102}Zr. The analysis of alignments and staggering in these bands indicates that they correspond to γ-soft and triaxial structures. This is the first such observation in Zr nuclei. The emergence of γ instability in Zr isotopes solves the puzzle of the sudden appearance of well-developed γ bands above $Z = 40$, in Mo and Ru nuclei.

One of the questions vividly discussed in recent works concerns the presence of surface vibrations in nuclei. In addition to questioning the presence of $K = 0$, β vibrations there are also doubts about the origin of $K = 2$, γ vibrations in nuclei (see reviews by Garrett [36] and Sharpey-Schafer [37]). The observation in this work of two $K^\pi = 2^+$ bands in ^{102}Zr with their bandheads well within the pairing gap, one of which shows features of a triaxial structure and the other of a γ soft vibrator, suggests that there is room for γ vibrations, though as mentioned above, mixing between the two as well as with 2-qp structure has to be considered [34].

ACKNOWLEDGMENTS

This material is based upon work supported by the US Department of Energy, Office of Science, Office of Nuclear Physics, under Contract No. 1 DE-AC02-06CH11357. The authors are indebted for the use of ^{248}Cm to the Office of Basic Energy Science, U.S. Department of Energy, through the transplutonium element production facilities at the Oak Ridge National Laboratory.

[1] E. Chiefetz, R. C. Jared, S. G. Thompson, and J. B. Wilhelmy, Phys. Rev. Lett. **25**, 38 (1970).
[2] W. Urban, T. Rząca-Urban, J. Wiśniewski, I. Ahmad, A. G. Smith, and G. S. Simpson, Phys. Rev. C **99**, 064325 (2019).
[3] W. Urban, T. Rząca-Urban, A. Złomaniec, G. Simpson, J. L. Durell, W. R. Phillips, A. G. Smith, B. J. Varley, I. Ahmad, and N. Schulz, Eur. Phys. J. A **16**, 11 (2003).
[4] J. K. Hwang, A. V. Ramayya, J. H. Hamilton, D. Fong, C. J. Beyer, P. M. Gore, Y. X. Luo, J. O. Rasmussen, S. C. Wu, I. Y. Lee, C. M. Folden, III, P. Fallon, P. Zielinski, K. E. Gregorich, A. O. Macchiavelli, M. A. Stoyer, S. J. Asztalos, T. N. Ginter, S. J. Zhu, J. D. Cole, G. M. Ter Akopian, Y. T. Oganessian, and R. Donangelo, Phys. Rev. C **67**, 054304 (2003).
[5] W. Urban, J. A. Pinston, J. Genevey, T. Rząca-Urban, A. Złomaniec, G. Simpson, J. L. Durell, W. R. Phillips, A. G. Smith, B. J. Varley, I. Ahmad, and N. Schulz, Eur. Phys. J. A **22**, 241 (2004).
[6] A. Złomaniec, H. Faust, J. Genevey, J. A. Pinston, T. Rząca-Urban, G. S. Simpson, I. Tsekhanovich, and W. Urban, Phys. Rev. C **72**, 067302 (2005).
[7] K. Heyde and J. L. Wood, Rev. Mod. Phys. **83**, 1467 (2011).
[8] N. Gavrielov, A. Leviatan, and F. Iachello, Phys. Rev. C **99**, 064324 (2019).
[9] P. Spagnoletti, G. Simpson, S. Kisyov, D. Bucurescu, J.-M. Régis, N. Saed-Samii, A. Blanc, M. Jentschel, U. Köster, P. Mutti, T. Soldner, G. de France, C. A. Ur, W. Urban, A. M. Bruce, C. Bernards *et al.*, Phys. Rev. C **100**, 014311 (2019).
[10] S. Miyahara and H. Nakada, Phys. Rev. C **98**, 064318 (2018).
[11] J. K. Hwang, A. V. Ramayya, J. H. Hamilton, J. O. Rasmussen, Y. X. Luo, D. Fong, K. Li, C. Goodin, S. J. Zhu, S. C. Wu, M. A. Stoyer, R. Donangelo, X.-R. Zhu, and H. Sagawa, Phys. Rev. C **74**, 017303 (2006).
[12] F. Browne, A. M. Bruce, T. Sumikama, I. Nishizuka, S. Nishimura, P. Doornenbal, G. Lorusso, P.-A. Sderstrm, H. Watanabe, R. Daido, Z. Patel, S. Rice, L. Sinclair, J. Wu, Z. Y. Xu *et al.*, Phys. Rev. C **96**, 024309 (2017).
[13] A. Guessous, N. Schulz, W. R. Phillips, I. Ahmad, M. Bentaleb, J. L. Durell, M. A. Jones, M. Leddy, E. Lubkiewicz, L. R. Morss, R. Piepenbring, A. G. Smith, W. Urban, and B. J. Varley, Phys. Rev. Lett. **75**, 2280 (1995).
[14] A. G. Smith, J. L. Durell, W. R. Phillips, M. A. Jones, M. Leddy, W. Urban, B. J. Varley, I. Ahmad, L. R. Morss, M. Bentaleb, A. Guessous, E. Lubkiewicz, N. Schulz, and R. Wyss, Phys. Rev. Lett. **77**, 1711 (1996).
[15] J. A. Shannon, W. R. Phillips, J. L. Durell, B. J. Varley, W. Urban, C. J. Pearson, I. Ahmad, C. J. Lister, L. R. Morss, K. L. Nash, C. W. Williams, N. Schulz, E. Lubkiewicz, and M. Bentaleb, Phys. Lett. B **336**, 136 (1994).
[16] K. Sieja, F. Nowacki, K. Langanke, and G. Martínez-Pinedo, Phys. Rev. C **79**, 064310 (2009).

[17] P. J. Nolan, F. A. Beck, and D. B. Fossan, Annu. Rev. Nucl. Part. Sci. **44**, 561 (1994).
[18] I.-Yang Lee, Nucl. Phys. A **520**, c641 (1990).
[19] W. Urban, M. Czerwinski, J. Kurpeta, T. Rzaca-Urban, J. Wisniewski, T. Materna, L. W. Iskra, A. G. Smith, I. Ahmad, A. Blanc, H. Faust, U. Koster, M. Jentschel, P. Mutti, T. Soldner, G. S. Simpson, J. A. Pinston, G. deFrance, C. A. Ur, V. V. Elomaa, T. Eronen, J. Hakala, A. Jokinen, A. Kankainen, I. D. Moore, J. Rissanen, A. Saastamoinen, J. Szerypo, C. Weber, and J. Aysto, Phys. Rev. C **96**, 044333 (2017).
[20] D. Patel, A. G. Smith, G. S. Simpson, R. M. Wall, J. F. Smith, O. J. Onakanmi, I. Ahmad, J. P. Greene, M. P. Carpenter, T. Lauritsen, C. J. Lister, R. F. Janssens, F. G. Kondev, D. Seweryniak, B. J. P. Gall, O. Dorveaux, and B. Roux, J. Phys. G: Nucl. Part. Phys. **28**, 649 (2002).
[21] K. Li, J. H. Hamilton, A. V. Ramayya, S. J. Zhu, Y. X. Luo, J. K. Hwang, C. Goodin, J. O. Rasmussen, G. M. Ter-Akopian, A. V. Daniel, I. Y. Lee, S. C. Wu, R. Donangelo, J. D. Cole, W. C. Ma, and M. A. Stoyer, Phys. Rev. C **78**, 044317 (2008).
[22] B. Singh, Nucl. Data Sheets **109**, 297 (2008).
[23] H. Naidja, F. Nowacki, B. Bounthong, M. Czerwinski, T. Rząca-Urban, T. Roginski, W. Urban, J. Wiśniewski, K. Sieja, A. G. Smith, J. F. Smith, G. S. Simpson, I. Ahmad, and J. P. Greene, Phys. Rev. C **95**, 064303 (2017).
[24] I. Ahmad and W. R. Phillips, Rep. Prog. Phys. **58**, 1415 (1995).
[25] H. Hua, C. Y. Wu, D. Cline, A. B. Hayes, R. Teng, R. M. Clark, P. Fallon, A. Goergen, A. O. Macchiavelli, and K. Vetter, Phys. Rev. C **69**, 014317 (2004).
[26] J. L. Durell, W. R. Phillips, C. J. Pearson, J. A. Shannon, W. Urban, B. J. Varley, N. Rowley, K. Jain, I. Ahmad, C. J. Lister, L. R. Morss, K. L. Nash, C. W. Williams, N. Schulz, E. Lubkiewicz, and M. Bentaleb, Phys. Rev. C **52**, R2306 (1995).
[27] J. L. Durell, T. J. Armstrong, and W. Urban, Acta Phys. Pol. B **34**, 2277 (2003).
[28] W. Urban, J. L. Durell, W. R. Phillips, A. G. Smith, M. A. Jones, I. Ahmad, A. R. Barnett, M. Bentaleb, S. J. Dorning, M. J. Leddy, E. Lubkiewicz, L. R. Morss, T. Rząca-Urban, R. A. Sareen, N. Schulz, and B. J. Varley, Z. Phys. A **358**, 145 (1997).
[29] M. A. Jones, W. Urband, and W. R. Phillips, Rev. Sci. Instrum. **69**, 4120 (1998).
[30] W. Urban, R. M. Lieder, W. Gast, G. Hebbinghaus, A. Kreämer-Flecken, K. P. Blume, and H. Hübel, Phys. Lett. B **185**, 331 (1987).
[31] R. F. Casten, *Nuclear Structure From a Simple Perspective* (Oxford University, Oxford, 1990).
[32] N. V. Zamfir and R. F. Casten, Phys. Lett. B **260**, 265 (1991).
[33] E. A. McCutchan, D. Bonatsos, N. V. Zamfir, and R. F. Casten, Phys. Rev. C **76**, 024306 (2007).
[34] K. Nomura, N. Shimizu, D. Vretenar, T. Nikšić, and T. Otsuka, Phys. Rev. Lett. **108**, 132501 (2012).
[35] D. De Frenne, Nucl. Data Sheets **110**, 1745 (2009).
[36] P. E. Garrett, J. Phys. G: Nucl. Part. Phys. **27**, R1 (2001).
[37] J. Sharpey-Schafer, R. A. Bark, S. P. Bvumbi, T. R. S. Dinoko, and S. N. T. Majola, Eur. Phys. J. A **55**, 15 (2019).